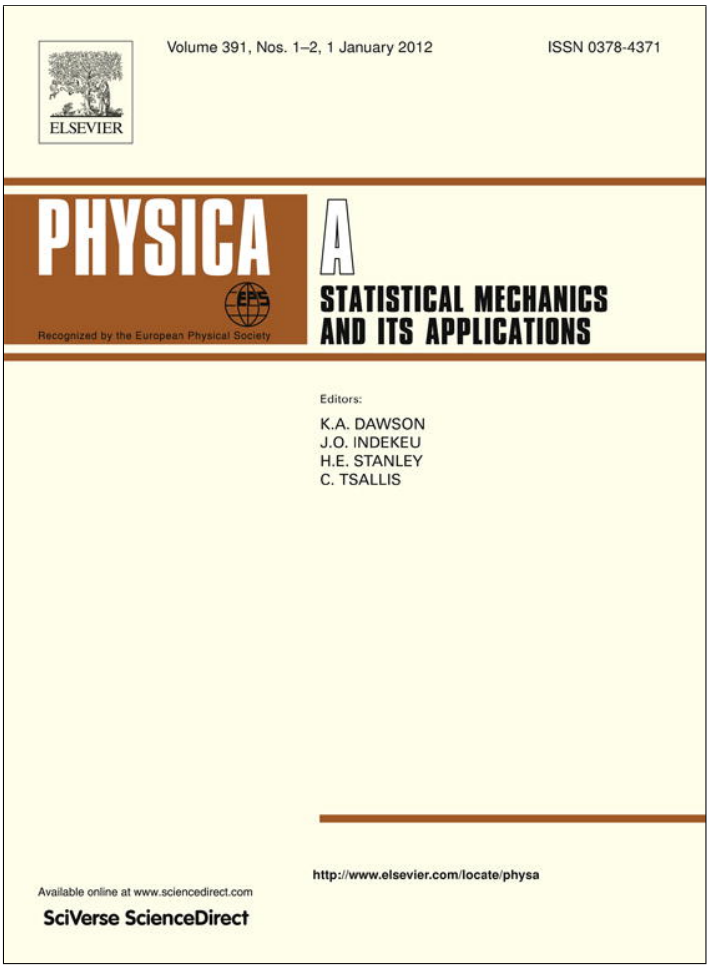

Physica A 391 (2012) 170–179

Contents lists available at SciVerse ScienceDirect

Physica A

journal homepage: www.elsevier.com/locate/physa

Detecting switching points using asymmetric detrended fluctuation analysis

Miguel A. Rivera-Castro [a], José G.V. Miranda [a], Daniel O. Cajueiro [b,c], Roberto F.S. Andrade [a,c,*]

[a] Instituto de Física, Universidade Federal da Bahia, BA 40210-340, Brazil
[b] Department of Economics – University of Brasilia, DF, 70910-900, Brazil
[c] National Institute of Science and Technology for Complex Systems, Brazil

ARTICLE INFO

Article history:
Received 5 May 2011
Received in revised form 5 July 2011
Available online 30 July 2011

Keywords:
Switching points
Asymmetric fluctuations
Local detrended analysis
Financial series

ABSTRACT

This work uses the concept of Asymmetric Detrended Fluctuation Analysis (A-DFA) to investigate and characterize the occurrence of trend switching in financial series. A-DFA introduces two new roughness exponents, H^+ and H^-, which differ from the usual one H by separately taking into account contributions to the fluctuations according to whether the local trend is, respectively, upward or downward. The developed methodology requires the evaluation of local values of $H(t)$, $H^+(t)$, and $H^-(t)$, by restricting the size of the largest window around the value t. We show that $H^+(t)$ and $H^-(t)$ behave differently in the neighborhoods of switching points (SPs) where trends change sign. Properly taken differences between shifted local values of $H(t)$, $H^+(t)$, and $H^-(t)$ allow to identify and characterize SP's. Tests with Weiertrasse functions, isolated peaks, and actual financial series are presented, supporting the validity of the proposed method.

1. Introduction

Within the broad framework provided by statistical physics, it has been recognized that financial markets are typical complex systems, with a large number of agents with different perspectives and conflicting interests, affected by large number of random, time dependent information input arising from any country in the world [1–3]. The fact that the forces acting on the market are of different nature and that small disturbances may result in large effects is responsible for the stochastic nature of this system and for its complexity. The large amount of actual data provided by the market records together with their importance for everyone's daily life have turned financial markets into paradigmatic systems, being currently applied to develop useful tools to measure, understand and, if possible, predict the dynamics of complexity [4–6].

Price fluctuations in stock market records constitute primary economic information source [7,8] that have been thoroughly investigated for the purpose of understanding specific features of economic dynamics, among which the trend for persistent rise or fall of prices changes. Preis and Stanley [9–12] have enlarged this perspective for any generic complex systems, introducing the concept of *switching points* (SPs) to characterize such events in a more precise way, by stating that such trend changes occur in an abrupt and almost discontinuous way. In the specific case of financial markets, switching events creating upward trends ("bubbles") and downward trends ("financial collapse") have been fairly common in the past three decades [13,4,5]. This change occurs at scale times ranging from macroscopic bubbles persisting for hundreds of days to microscopic bubbles persisting for only seconds.

* Corresponding author at: Instituto de Física, Universidade Federal da Bahia, BA 40210-340, Brazil. Tel.: +55 71 32337518.
E-mail addresses: marc@ufba.br (M.A. Rivera-Castro), vivas@ufba.br (J.G.V. Miranda), danielcajueiro@unb.br (D.O. Cajueiro), randrade@ufba.br (R.F.S. Andrade).

0378-4371/$ – see front matter © 2011 Elsevier B.V. All rights reserved.
doi:10.1016/j.physa.2011.07.009

According to the original definition, an SP event, at a specific instant of time t_i within a complex system record $y(t)$, is identified by a very large value of the return variance within a local window around t_i [10]. The magnitude of such events can vary over many time scales that depend on a precise definition of "large" and of the window width L and, as such, a comprehensive approach for SP deserves careful analyses. On the other hand, we think it is important to investigate whether other features present in the records can be used to detect SPs. In this work, we develop an approach for SP identification and characterization based on the *asymmetric detrended fluctuation analysis* method [14] (A-DFA). It has been devised to identify different fluctuation properties of presumed non-stationary series, by identifying and separating fluctuation contributions according to the upward or downward character of the local trend. If the fluctuations are casted into two groups according to different trends at all scales, it is possible to define two new scaling exponents, say H^+ and H^-. If the series is symmetric with respect to the trends, both H^+ and H^- are equal to the usual roughness (or Hurst) exponent H. If this property is not observed, the method assigns a measurable asymmetric character to the series.

To extend this idea for SP identification, we develop a local A-DFA evaluation procedure. Namely, we couple A-DFA with a sliding window procedure, which amounts to evaluating local exponents $H(t)$, $H^+(t)$ and $H^-(t)$. As we will discuss, it happens that the set of three local roughness exponents allows to characterize, in qualitative and quantitative ways, the emergence of sudden changes in the time records that we identify as SPs. The method happens to be robust with respect to the width of the sliding window, provided it remains small enough to be considered local and large enough to include sufficient points for the DFA analysis.

This paper is further organized as follows. In Section 2, we indicate the most important steps for the A-DFA procedure, in such a way to provide an easy-to-follow receipt on how the results have actually been obtained. Section 3 is divided into two subsections, where we discuss, respectively, results for series generated with specific algorithms warranting specific scaling properties, and on price series from stock markets. Finally, Section 4 presents our concluding remarks and discussions.

2. Local asymmetric detrended fluctuation analysis

DFA is a reliable method for the evaluation of the roughness exponent H of a stationary random time series. In its original and most used form [15,16], linear trends are eliminated from the series by calculating fluctuations around the best straight line segment in a box of length n. Generalized versions of the original idea have been proposed, in which trends represented by higher polynomial order q (DFAq) can be eliminated [17] or, alternatively, detrended multi-fractal analyses of non-stationary series can be performed [18]. In recent works [19,20], the idea of detrending was enlarged in a different context, namely, taking into account the mutual influence of two time series by defining the detrended cross-correlation analysis. It has also been shown that, by working with polynomials of degree q, periodic trends in data have been eliminated in the cross-correlation analysis [21]. The common feature in any detrending algorithm is quite useful as it allows to eliminate trends in many scale regions that are mostly reflecting the global adjustment of the system to some external parameter variations rather than reflecting the intrinsic dynamic properties of the system.

If we start with a series of equidistant time increments $\{x(t)\}$, $t = 1, \ldots, N$, we can obtain the path (or the profile)

$$y(t) = \sum_{j=1}^{t} x(t). \tag{1}$$

The entire interval $[1, N]$ can be divided into a series of M_n boxes of length n, not necessarily self-excluding. Each of such boxes receives a label (m, n), $m = 1, \ldots, M_n$. In our calculations, we considered a certain level of overlap between the boxes for the purpose of increasing the number of boxes where the method is applied and, hence, to improve the statistics.

To evaluate the magnitude of fluctuations in the box (m, n) and, concomitantly, eliminate the trend of order q, we consider the difference

$$y_s(t) = y(t) - p_q(t; (m, n)), \tag{2}$$

where $p_q(t; (m, n))$ represents the polynomial of order q that minimizes the sum of $y_s(t)^2$ when t spans all points of the considered box. To be more precise, we consider the residue

$$f(m, n) = \frac{1}{n} \sum_{j=I_{\min}(m,n)}^{I_{\max}(m,n)} y_s^2(j), \tag{3}$$

where $I_{\min}(m, n)$ and $I_{\max}(m, n)$ are the lower and upper limit of the (m, n) box. When $q = 0$, $f(m, n)$ corresponds to the roughness function $W(m, n)$ of the (m, n) box. Subsequently, we have the average

$$F(n) = \left[\frac{1}{M_n} \sum_{m=1}^{M_n} f(m, n) \right]^{1/2}, \tag{4}$$

which expresses the average detrended roughness at length scale n of the entire profile. If the original series presents long-range correlations, it is expected that the values of $F(n)$ follows a power law

$$F(n) \sim n^H, \tag{5}$$

where the roughness exponent $H = 1 - \gamma/2$ is related to the exponent describing the decay of the correlation function $C(j) = \langle y(t)y(t+j)\rangle \sim j^{-\gamma}$, and $\langle\ \rangle$ represents the series average. In the current work, as we proceed with the investigation of economic and financial data, $y(t)$ represents the logarithm of the price or the market index in the original series.

The A-DFAq variant proposed by Alvarez-Ramirez et al. [14] aims to characterize correlations in non stationary asymmetric time series, so that two further exponents H^+ and H^- can inform on the scaling properties when the series trends are upwards or downwards. The basic idea is to cast the sums in (3) into two classes according to the trend property of the (m, n) box. For this purpose, some extra steps must be added to usual DFAq framework sketched above. So we consider also

$$x_s(t) = x(t) - r_1(t; (m, n)), \tag{6}$$

where $r_1(t; (m, n))$, in a similar way as $p_q(t; (m, n))$, represents the linear function that minimizes the sum of $x_s(t)^2$ when t spans all points of the considered box. It is clear that $r_1(t) = ct + d$, with c and d box dependent constants. The set of all (m, n) boxes can be divided into two subsets B^+ B^- according to the box trend, i.e., to the signal of c on that box. Therefore, we will consider two new functions

$$F(n)^{\pm} = \left[\frac{1}{M_n^{\pm}} \sum_{(m,n)\in B^{\pm}} f(m, n)\right]^{1/2}. \tag{7}$$

In (7), $M_n^{\pm}$ counts the number of boxes in the $B^{\pm}$ subsets. Finally, the asymmetric exponents $H^{\pm}$ can be defined if power law dependence between $F(n)^{\pm}$ and n is verified, i.e.,

$$F(n)^{\pm} \sim n^{H^{\pm}}. \tag{8}$$

The local A-DFAq combines the steps used for detecting the asymmetry between the upward and downward fluctuations with the proposals to detect local dependences of the roughness function $W(t)$ and exponent $H(t)$. Such local analyses have been widely used in the investigation of complex systems, ranging from econophysics [22–24] to seismic signals [25–27]. In this work, we used the sliding window procedure [28–30], with the particular value $q = 1$, to obtain the asymmetric local scaling properties of the considered series. This amount to replace the total number of points N used for the evaluation of the sums and exponents in Eqs. (3)–(7) by L, the width of the sliding window. At a given point t, the corresponding exponents $H(t)$, $H^+(t)$, and $H^-(t)$ will be evaluated by taking into account the set of $L + 1$ points, being $L/2$ points to the left and $L/2$ points to the right of point t.

It is important to recall the existence of a natural limit for event localization. Indeed, the evaluation of scaling exponents based on a neighborhood of width L is based on the slope of the linear fit of $\log F(n)$ with respect to n (see Eq. (8)), where n is usually restricted to $L/4$. If we require a minimum of 5 points to obtain a meaningful value of the slope, and consider that, on the average, half of the points are used to evaluate H^+ and H^-, then $L = 40$ appears as a lower bound of for the window width.

3. Results

The results in this section were devised, in first place, to test the method with well characterized stationary data series and single peak profiles. In the first case, it is expected that when we take into account trends with positive and negative signals in different ranges of time scale, global values of H^+ and H^- do not deviate from each other. On the other hand, local values $H^+(t)$ and $H^-(t)$ may differ from each other in a meaningful way. The use of single peak profile helps to illustrate the kind of response the method provides either to bare disturbance or in combination with a rough random substrate. In this respect, a superposition of such peak allows to artificially generate controlled switching events to basic random data. Once the validation, reliability, and limitation of the method have been assessed, it is used to explore actual data series of economic activity. These are subject to the influence of a large number of sudden and unexpected political and natural factors that modify the dynamics usually related to the economic related demand and offer of goods and services. In the two next subsections, we discuss specific details of each group of results.

3.1. Detecting switching events

In Fig. 1, we illustrate the implementation of the local A-DFA1 to the Weierstrass function $W_{0.5}(t)$ with 2500 points. As stated above, the dependence of all three functions $F(n)$, $F(n)^{\pm}$ on n shows a very precise linear dependence in the double-logarithmic plot with slope 0.5 when the whole data sample is considered (not shown). Fig. 1a and b show how $H_0(t)$, $H^+(t)$, and $H^-(t)$ depend on t when the analysis and evaluation is restricted to a sliding window of width $L = 100$. It is possible to note small fluctuations on the value of $H(t)$ around $H = 0.5$ related with a much smaller used statistics, but such fluctuations become smaller when the width of the sliding windows increases. We further observe that, for the same window width, the fluctuations on the values of $H^+(t)$ and $H^-(t)$ are undoubtedly larger than those of $H(t)$, and that they are overwhelmingly out of phase, i.e., when $H^+(t) > H(t)$ it is more likely that $H^-(t) < H(t)$ and vice-versa. In Fig. 1c, we draw the difference $H^+(t) - H^-(t)$ to show more clearly the out of phase feature.

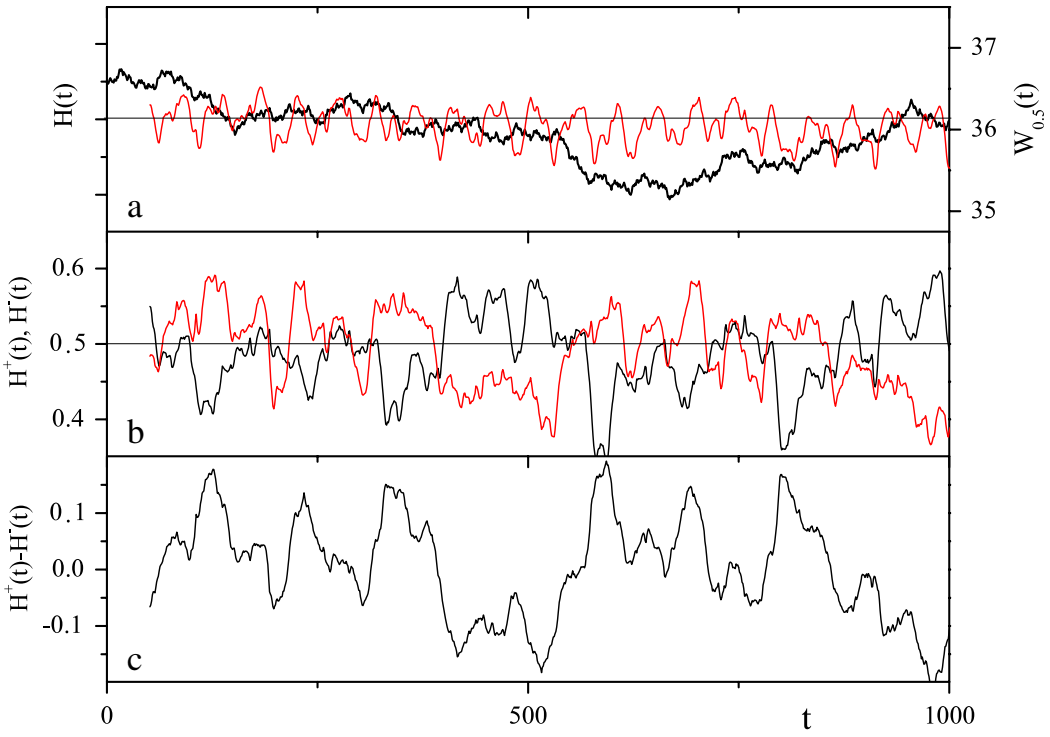

Fig. 1. Time dependency of a well known profile $W_{0.5}(t)$ (black) together with the corresponding local Hurst exponents $H(t)$ (red–gray) (a). In panel (b), the asymmetric Hurst exponents $H^+(t)$ (black) and $H^-(t)$ (red–gray) and, in (c), the difference $H^+(t) - H^-(t)$. (For interpretation of the references to colour in this figure legend, the reader is referred to the web version of this article.)

It becomes more convenient to illustrate the dependence of the exponents as a function of L in the case of two isolated peaks in a flat profile, as shown in Fig. 2a. The results in Fig. 2b show clearly that the values of H_i depend on L. In Fig. 2c, we illustrate the behavior of $H^+(t)$ and $H^-(t)$. Note that, if the peak is antisymmetric with respect to $t = 0$, we obtain $H^+(t) = H^-(-t)$. The superposition of an external peak to a random record leads also to very sharp changes in the values of $H^i(t)$ in the neighborhood of the peak, as shown in the second half of the profile in Fig. 2a–d. Special features for the isolated peak on the l.h.s include the following: the effect of L on the interval where $H^i(t)$ is non zero; a structured peak with the presence of several satellites; the displacement of the maxima of $H^i(t)$ with respect to the peak maxima. The most important feature for the superimposed peak on the r.h.s refers to an increase in the value of $H^i(t)$ in the region that depends on the σ and on L.

Fig. 2 makes it evident that, for the single peak, the maximum value attained by $H^i(t)$ does not coincide with the peak. This can be easily understood when we consider the evaluation of $H(t)$. Its maximum value corresponds to the instants of t such that the interval $[t-L/2, t+L/2]$ covers one side (ascending or descending) of the peak. To make the maximum of $H(t)$ coincide with the maximum of the peak it is necessary to shift the coordinate of $H(t)$ by $L/2$. To proceed in a symmetric way, we consider the combination $H(t-L/2)H(t+L/2) \equiv \overline{H}(t)$, as shown in Fig. 2d (red line). Note that the so defined value $\overline{H}(t)$ is the square of the geometrical average between $H(t-L/2)$ and $H(t+L/2)$. We have found out that such definition is more suitable for localizing SPs as they reduce the production of satellite peaks that are produced by the arithmetic average. The graphs show a good coincidence in the location of the peaks, but it still depends strongly on L. In Fig. 2d, we also show (black line) the difference between the shifted values $\overline{H}^{\pm}(t) \equiv H^{\pm}(t - L/2)H^{\pm}(t + L/2)$. Besides the agreement in the location of the peaks, we can also observe an enhancement of the magnitude. This is caused by the fact that, when the peak reaches its local minimum, $\overline{H}^{+}$ also attains a local minimum and $\overline{H}^{-}$ a local maximum. On the contrary, when the peak reaches a local maximum the value of $\overline{H}^{-}$ reaches a local minimum and $\overline{H}^{+}$ a local maximum.

The shift in the value of the argument of $H^i(t)$ provides a good agreement with the extreme position in single peak situations, but the situation of random series deserves a further discussion. The discussion above applies with some restrictions. Let us observe that, since the series fluctuates randomly, local minima and maxima may occur in a variety of ways: embedded in a neutral trend patch, at the beginning or at the end of the persistent trend patch, and so on. Therefore, the combination of all these factors lead to the fact that, depending on L, many local extreme points do follow this rule, but some fail to satisfy them. Another empirically observed interesting effect is that the behavior of $H^i(t)$ becomes similar to that of $\overline{H}^i(t)$, as one can observe from the results in the r.h.s of Fig. 2c.

The effect of shifting the arguments of the exponents for the purpose of getting a good correspondence with the location of the peaks becomes quite evident in the combinations $\overline{H}^{+}(t) - \overline{H}^{-}(t)$ and $2\overline{H}(t) - \overline{H}^{+}(t) - \overline{H}^{-}(t)$, which can be regarded as the subtraction and sum of $\overline{H}^{\pm}(t) - \overline{H}(t)$. This is shown in Fig. 3a and b. There we show that local extreme of $W_{0.5}$ frequently

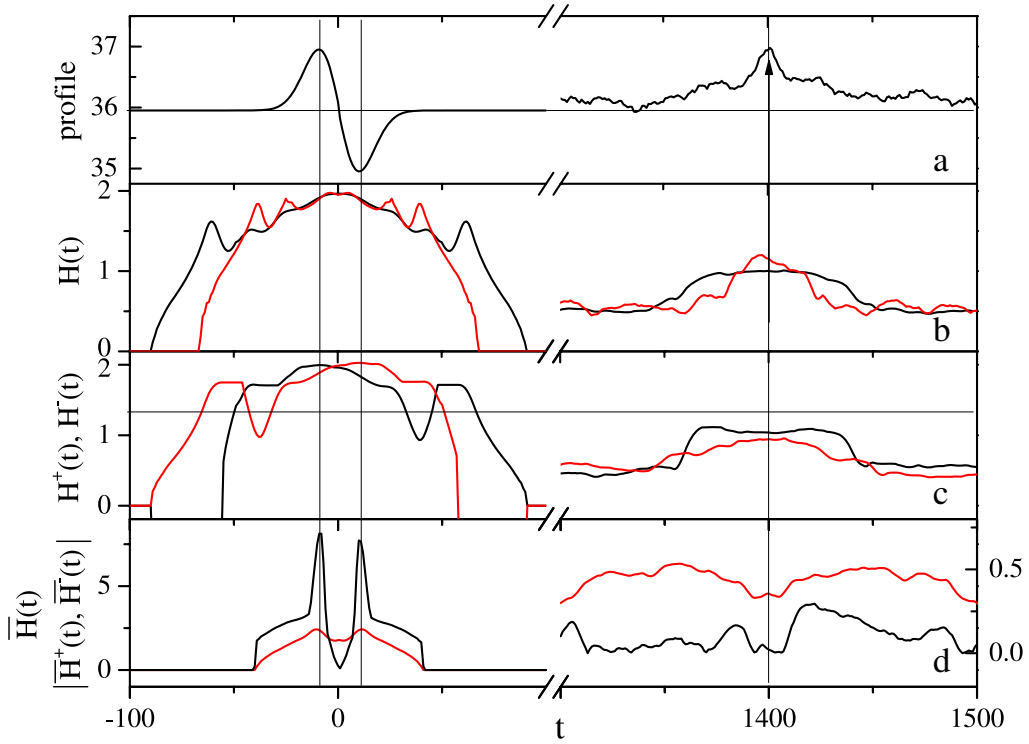

Fig. 2. Dependence of local $H^i(t)$ on the window size L for deterministic profiles: in panel (a), we consider a peak given by the derivative of a Gaussian curve with variance $\sigma = 15$ (l.h.s), together with a Gaussian peak of variance $\sigma = 12$ superimposed on the same $W_{0.5}(t)$ profile (indicated by an arrow in the r.h.s). In (b), the usual $H(t)$ with window widths $L = 60$ (black) and $L = 100$ (red–gray). For the sake of a clearer picture, in (c) we draw only the curves for $H^+(t)$ (black) and $H^-(t)$ (red–gray) when $L = 100$. (For interpretation of the references to colour in this figure legend, the reader is referred to the web version of this article.)

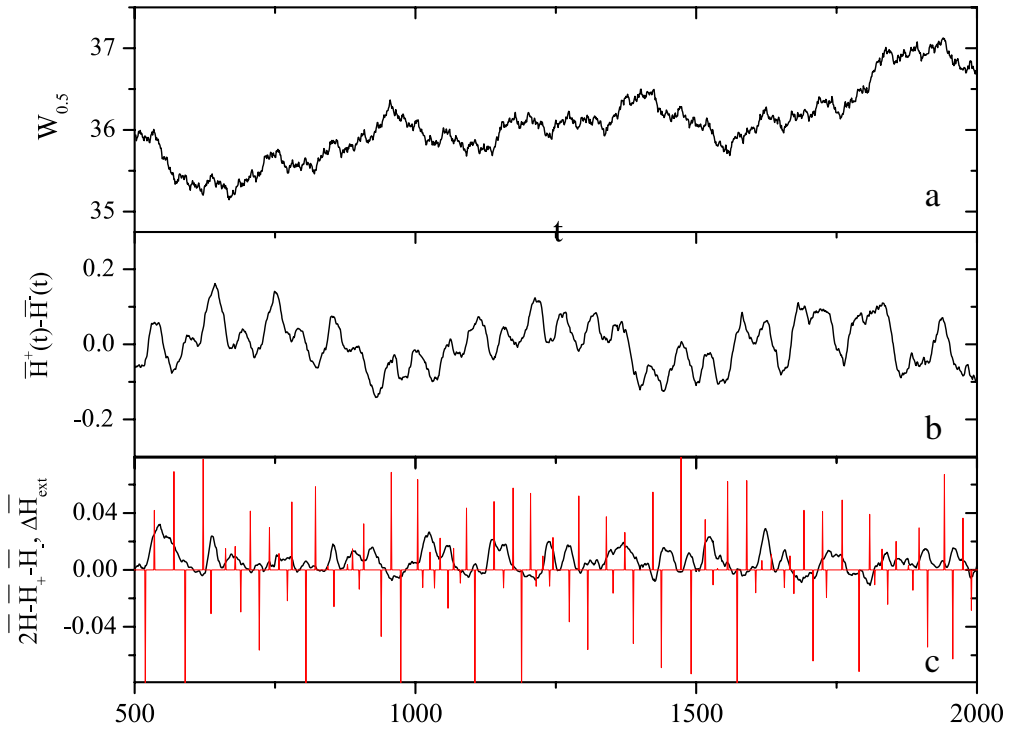

Fig. 3. Dependence of the shifted combinations $\overline{H}^+(t) - \overline{H}^-(t)$ (b) and $2\overline{H}(t) - \overline{H}^+(t) - \overline{H}^-(t)$ (c) for the $W_{0.5}(t)$ profile (a). It is possible to notice a quite nice agreement in SPs on (a) with the extreme values in (b) and (c). In (c), we included the extreme values $\Delta\overline{H}$ obtained by the procedure described in the text.

occur together with extreme of $\overline{H}^+(t) - \overline{H}^-(t)$. Note that, depending on $\overline{H}^+(t)$ being larger or smaller than $\overline{H}^-(t)$ and the relation about the minimum or maximum values of the record with minimum or maximum values of $\overline{H}^{\pm}(t)$, the magnitude

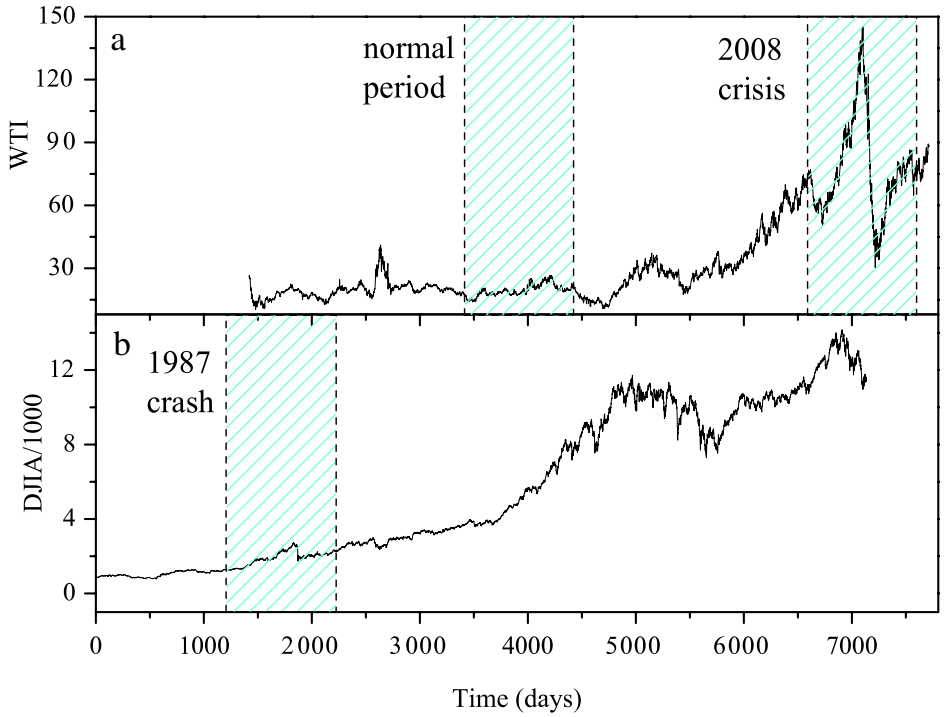

Fig. 4. WTI (a) and DJIA (b) time evolution with the indication of the periods that are subject to a closer analysis in Figs. 6–8.

of extreme values of $\overline{H}^+(t) - \overline{H}^-(t)$ are enhanced in the following conditions: (a) the extreme is a maximum and $\overline{H}^+ > \overline{H}^-$; (b) the extreme is a minimum and $\overline{H}^+ < \overline{H}^-$. On the other hand, the magnitude is depleted in opposite conditions: (a) the extreme is a maximum and $\overline{H}^+ < \overline{H}^-$; (b) the extreme is a minimum and $\overline{H}^+ > \overline{H}^-$.

The smoother sign provided by $2\overline{H} - \overline{H}^+ - \overline{H}^-$ offer a further possibility to identify SPs. Fig. 3c shows that these two desired features are present herein. Nevertheless, the magnitudes of maxima and minima are subject to the same restrictions pointed out for the curve $\overline{H}^+ - \overline{H}^-$.

These features bring some difficulties if one wants to associate the magnitude of the extreme values to that of the switching points. So let us discuss the method we developed to minimize this asymmetric effect. First, we use a procedure to locate SPs in the two series $\overline{H}^+ - \overline{H}^-$ and $2\overline{H} - \overline{H}^+ - \overline{H}^-$, although it can be used in any time series $y(t)$ and extract local maxima and minima. The output is a new series $z(t)$. We may choose the width ℓ of the interval of contiguous points used to decide whether a point $(\bar{t}, y(\bar{t}))$ is an extreme or not. It is a local maximum only if $y(\bar{t} - j) < y(\bar{t}) > y(\bar{t} + j)$ for $0 < j \leq \ell$ If $y(t)$ is not an extreme, what is observed for the large majority of values of t, we set $z(t) = 0$. If it is an extreme, we select this specific value of t and identify it as T_i. Then we set $z(i) = y(T_i - 1) - 2y(T_i) + y(T_i + 1)$. This procedure allows the identification of extreme based only on a local analysis, and that the magnitude of $z(i)$ takes into account the values of three contiguous extreme values of $y(T)$. This way the asymmetry in the magnitude of $\overline{H}^+ - \overline{H}^-$ and $2\overline{H} - \overline{H}^+ - \overline{H}^-$ will be reduced. The spikes in Fig. 3c identify the values $z(t_i) \to \Delta\overline{H}$ detected by the described procedure. Note that larger values of ℓ imply that detected SPs follow after larger patches of coherent ascending and descending trends detected by the values of exponents $\overline{H^i}$, and that the value of $z(i)$ may be also affected by the value of ℓ.

This procedure also opens the possibility for gauging the strength of an SP by the corresponding $z(t_i)$ value. Indeed it is quite natural to use the condition $|z(t_i)| > z_c$, where z_c takes into account the typical order of magnitude of the series $z(t_i)$, to decide whether a point $y(t_i)$ is an SP or not. This criterion will be used in the next subsection with the analysis of actual economic series.

3.2. Switching events in actual series

The methods described in the former subsection have been applied to two well known economic series: Dow Jones Industrial Average (DJIA) and West Texas Intermediate (WTI), which reflects the oil price fluctuations, being more sensitive to global political events that influence the market behavior of this commodity. In Fig. 4, we illustrate the time dependence of both series: DJIA from 23/05/1980 to 25/08/2008, and WTI from 02/01/1986 to 14/12/2010. The complete series were first used for the purpose of investigating the frequency and magnitude of SP events with respect to the values of ℓ and L. However, since they are quite large, we concentrated our qualitative analyses to three distinct periods: (i) from 1985 to 1988, encompassing the October 1987 crash (Oct87, with DJIA); (ii) a period corresponding to the relative stable oil price years 1994–1997 after the Gulf war (94–97, with WTI); (iii) and the sustained oil price increasing period that started in 2006 until 2009, containing the 2008 world economic crash (with WTI).

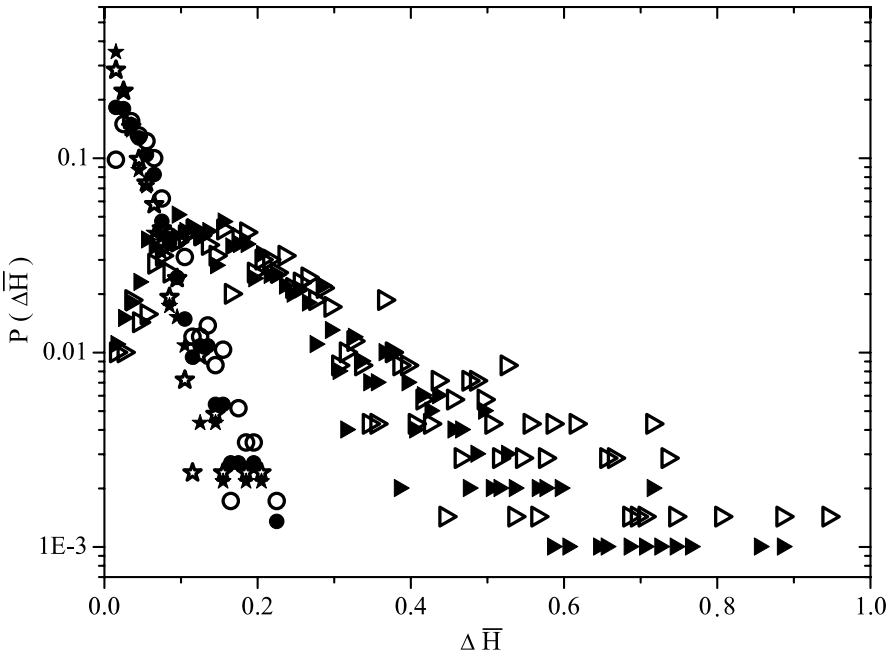

Fig. 5. Probability distribution of the magnitude of SP events in DJIA series (measured by $\Delta\overline{H}$) for several values of Ł and ℓ. Symbols indicate different (L, ℓ) pairs as indicated: solid right triangles (40, 5); solid circles (80, 5); solid stars (120, 5); hollow right triangles (40, 8); hollow circles (80, 8); hollow stars (120, 9). The distribution is little sensitive to the value of ℓ, but not on L.

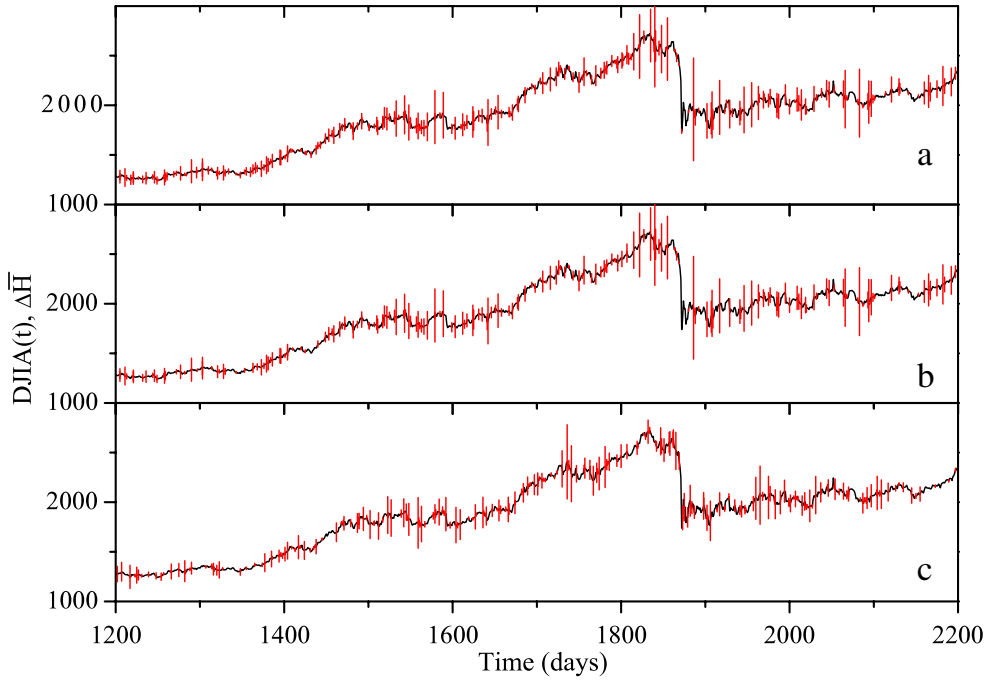

Fig. 6. DJIA time evolution encompassing the 1987 crisis (solid line) together with SP location discussed in the text (error bars) for $L = 40$, 80, and 120. In (a), $\Delta\overline{H}_c = 0$ while in (b) and (c) $\Delta\overline{H}_c = e^{-1}$. $\ell = 8$ in panels (a) and (b), and $\ell = 5$ in panel (c).

In Fig. 5, we show how the probability distribution $P(\Delta\overline{H})$ depends on $\Delta\overline{H}$ for some typical values of $L = 40$, 80, and 120, while $\ell = 5$ and 9. For all cases, we consider $z_c = \Delta\overline{H}_c = e^{-1}\langle\Delta\overline{H}\rangle$. The six curves show that the frequency decay exponentially with respect to the magnitude of $\Delta\overline{H}$. As expected, the total number of events (respectively, 995, 739, and 460, for $\ell = 5$ and $L = 40$, 80, and 120, and 698, 580, and 415, for $\ell = 8$ and $L = 40$, 80, and 120) decreases when the restrictions imposed on the definition (L and ℓ) increase. The same behavior is observed if we restrict the value of $\Delta\overline{H}_c$. Exponential decrease on the magnitude of events is also obtained with the original SP definition based on the local behavior of the variance [9,10,31].

Fig. 6 illustrates the location of the SPs on the Oct87 period. The full line indicates the time series, while error bars locate the values of t_i with SP events. The error bar length is proportional to the magnitude of $\Delta\overline{H}$ and, in all panels, we include

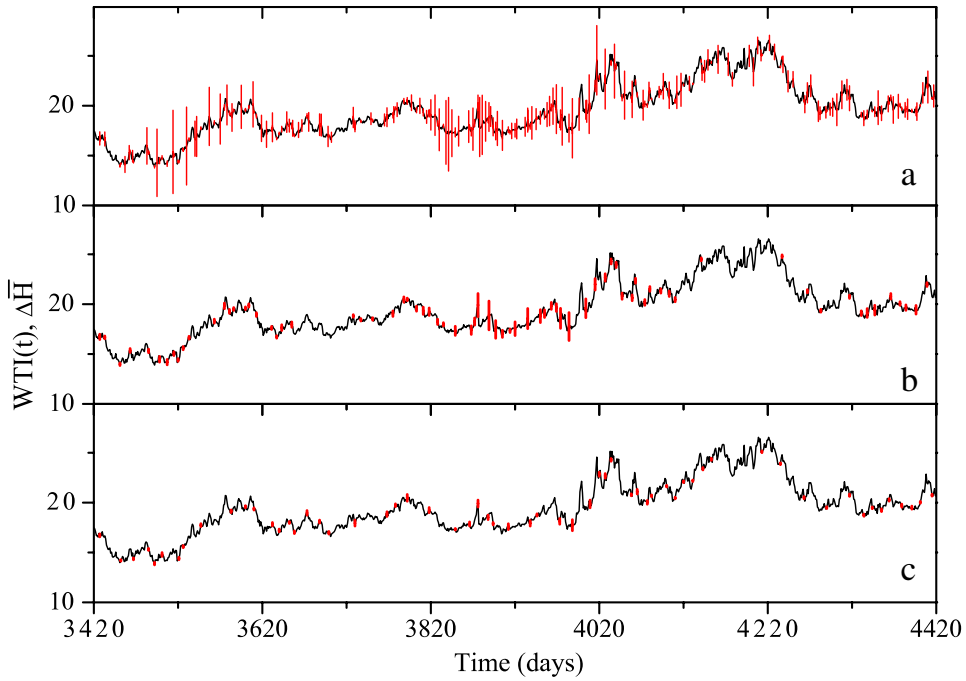

Fig. 7. WTI time evolution and SP localization in the 1993–1995 period. Different panels illustrate the dependence of SP localization as a function of L, for fixed $\ell = 5$ and $\Delta\overline{H}_c = e^{-1}$. Panel (a) includes of SPs detected with $L = 40$, 80, and 120. In (b) and (c) only SPs detected with $L = 40$ and 120, respectively. Not only the frequency of events decreases when L increases, but also the magnitude of $\Delta\overline{H}$.

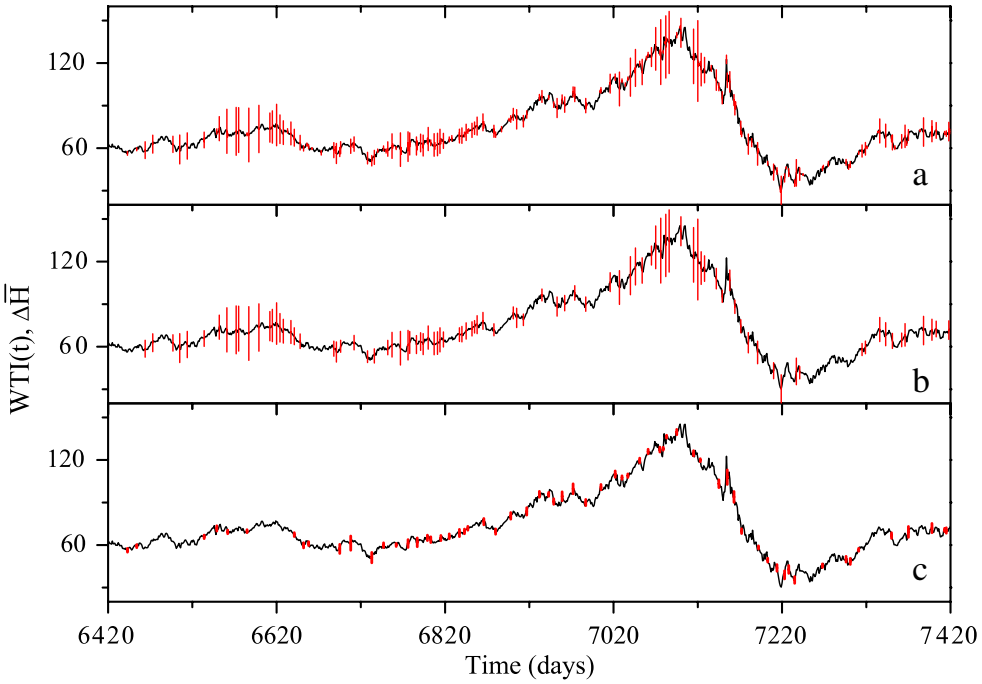

Fig. 8. Similar curves as shown in Fig. 7, but for the 2006–2008 period. Fixed values of $\ell = 5$ and $\Delta\overline{H}_c = e^{-1}$. In panel (a), SPs detected with $L = 40$, 80, and 120. In (b) and (c) only SPs detected with $L = 40$ and 80, respectively. As in Fig. 7, a similar decrease in the frequency and in the magnitude of events is observed when results for $L = 40$ and 80 are compared. This hints that small values of L are required for a more precise location of events.

three distinct values of $L = 40$, 80, and 120. In Fig. 6(a), we set $\ell = 8$ and $\Delta\overline{H}_c = 0$. By visual inspection, it is possible to notice that almost all sharp peaks that are natural candidates for SP events have been detected by the developed procedure. Fig. 6b shows that the number of occurrences decreases when we consider $\Delta\overline{H}_c = e^{-1}\langle\Delta\overline{H}\rangle$, but the most important SP events are preserved. Note that such decrease is more perceivable in the regions where fluctuations are not so large. Finally, in accordance with the results in Fig. 5, the number of SPs increases as ℓ decreases, as displayed in panel (c) for $\ell = 5$.

In Fig. 7, we stress the dependency of the location of SPs on L, for the 94–97 period. $\ell = 5$ is held constant for all cases. In (a), we include three distinct values of $L = 40$, 80, and 120, while panels (b) and (c) correspond to $L = 40$ and 120. The smaller number of SPs in (c) is in accordance with the previous results. Notice, however, that some more pronounced

extreme SPs that have been not detected by $L = 40$ scanning have been included when the window is wider. A comparison with the results in Fig. 6 shows that the variation in the magnitude of the error bars is smaller, which can be explained by the absence of huge fluctuations in the time series in the considered interval.

Finally, we consider in Fig. 8 a mixed period characterized by a long and constant upward trend in the oil price that ended with the 2008 world crisis. Here again the method captures the majority of local fluctuations in both phases. Fixing $\ell = 5$ we show, in (a), results for the three window widths $L = 40$, 80, and 120, while in (b) and (c) we restrict to the smaller and intermediate values $L = 40$ and 80.

4. Conclusions

For the purpose of investigating SP occurrence in financial series, we adapted the concept of A-DFA to obtain local values $H^{\pm}(t)$ that provide information on the upward and downward trends. The very fact that $H^{\pm}$ distinguish distinct scaling behavior in periods with different trends suggested us to explore the potentiality of this methodology. Despite the fact that such measures identify basic changes in the series behavior, the analysis of isolated peaks suggested us to work with the product of shifted values $H^{\pm}(t \pm L/2)$. Indeed, the measures $\overline{H^{\pm}}(t)$ were able to identify SPs also in deterministic and actual series. The framework is sufficiently tunable, by a small number of parameters related to the widths L and ℓ, and event relative magnitude $\Delta\overline{H}_c$, so that it is possible to choose two independent length scales under which the system can be analyzed. The number and magnitude of detected SPs are related by the preselected values of the quoted three parameters, so that the more relevant events can be filtered accordingly.

Since the proposed method is more elaborated than just looking at the local neighborhood of the original series, we would like to stress that, for practical purposes, this flexibility and the new information it is able to provide seems to justify our approach. Let us also note that our analyses do not require to introduce time re-normalization between two extreme values, as used in Ref. [10,31]. Finally, we point out that the results of the developed method can be still more relevant in the analysis of data sets where the intrinsic persistent behavior of upward and downward patches is more distinct than those provided here. Although it is well known that the crashes usually proceed in much shorter scale building upward times, the obtained average values of $H^{\pm}(t)$ do not differ that much from each other.

Acknowledgments

This work was partially supported by the following Brazilian funding agencies: CAPES, FAPESB (through the PRONEX program), and CNPq (individual grants and the INCTI-SC program).

References

[1] P.J.N.F. Johnson, P.M. Hui, Financial Market Complexity: What Physics Can Tell Us About Market Behaviour, Oxford University Press, Oxford, 2003.
[2] F. Schweitzer, G. Fagiolo, D. Sornette, F. Vega-Redondo, A. Vespignani, D.R. White, Economic networks: the new challenges, Science 326 (2009) 422–425.
[3] F. Schweitzer, G. Fagiolo, D. Sornette, F. Vega-Redondo, D.R. White, Economic networks: what do we know and what do we need to know? Advances in Complex Systems 12 (2009) 407–422.
[4] D. Sornette, A. Johansen, Large financial crashes, Physica A 245 (1997) 411–422.
[5] D. Sornette, Why Stock Markets Crash: Critical Events in Complex Financial Systems, Princeton University Press, Princeton, 2003.
[6] R.N. Mantegna, H.E. Stanley, Introduction to Econophysics: Correlations and Complexity in Finance, Cambridge University Press, Cambridge, 2007.
[7] F.D. Foster, S. Viswanathan, Variations in trading volume, return volatility, and trading costs – evidence on recent price formation models, Journal of Finance 48 (1993) 187–211.
[8] L.H. Ederington, J.H. Lee, How markets process information – news releases and volatility, Journal of Finance 48 (1993) 1161–1191.
[9] T. Preis, H.E. Stanley, How to characterize trend switching processes in financial markets, APCTP Bulletin 23–24 (2009) 18–23.
[10] T. Preis, H.E. Stanley, Switching phenomena in a system with no switches, Journal of Statistical Physics 138 (2010) 431–446.
[11] T. Preis, H.E. Stanley, Econophysics approaches to large-scale business data and financial crisis, in: Ch. Trend Switching Process in Financial Markets, Springer, 2010, pp. 3–26.
[12] T. Preis, H.E. Stanley, Bubble trouble, Physics World 24 (2011) 29–32.
[13] D. Sornette, A. Johansen, J.P. Bouchaud, Stock market crashes, precursors and replicas, Journal of Physique I 6 (1996) 167–175.
[14] J. Alvarez-Ramirez, E. Rodriguez, J.C. Echeverria, A dfa approach for assessing asymmetric correlations, Physica A 388 (2009) 2263–2270.
[15] J.G. Moreira, J.K.L. DaSilva, S.O. Kamphorst, On the fractal dimension of self-affine profiles, Journal of Physics A 27 (1994) 8079–8089.
[16] C.K. Peng, S.V. Buldyrev, S. Havlin, M. Simons, H.E. Stanley, A.L. Goldberger, Mozaic organization of dna nucleotides, Physical Review E 49 (1994) 1685–1689.
[17] J.W. Kantelhardt, E. Koscielny-Bunde, H.H. Rego, S. Havlin, A. Bunde, Detecting long-range correlations with detrended fluctuation analysis, Physica A 295 (2001) 441–454.
[18] J.W. Kantelhardt, S.A. Zschiegner, E.K.-B.E , S. Havlin, A. Bunde, H.E. Stanley, Multifractal detrended fluctuation analysis of nonstationary time series, Physica A 316 (2002) 87–114.
[19] B. Podobnik, H.E. Stanley, Detrended cross-correlation analysis: a new method for analyzing two non-stationary time series, Physical Review Letters 100 (2008) 084102.
[20] B. Podobnik, D. Horvatic, A.M. Petersen, H.E. Stanley, Cross-correlations between volume change and price change, Proceedings of the National Academy of Sciences of USA 106 (2009) 22079–22084.
[21] D. Horvatic, H.E. Stanley, B. Podobnik, Detrended cross-correlation analysis for non-stationary time series with periodic trends, Europhysics Letters 94 (2011) 18007.
[22] T. Lux, Long-term stochastic dependence in financial prices: evidence from the german stock market, Applied Economic Letters 3 (1996) 701–706.
[23] T. DiMatteo, T. Aste, M.M. Dacorigna, Long-term memories of developed and emerging markets: using the scaling analysis to characterize their stage of development, Journal of Banking and Finance 29 (2005) 827–851.
[24] D.O. Cajueiro, B.M. Tabak, Testing for long-range dependence in world stock markets, Chaos, Solitons and Fractals 37 (2008) 918–927.

[25] R.F.S. Andrade, O. Oliveira, A.L. Cardoso, L.S. Lucena, F.E.A. Leite, M.J. Porsani, R.C. Maciel, Exploring self-affine properties in seismograms, Computational Geosciences 13 (2009) 155–163.
[26] F.J. Herrmann, Seismic facies characterization by scale analysis, Geophysics Research Letters 28 (2001) 3871.
[27] F.J. Herrmann, Seismic deconvolution by atomic decomposition: a parametric approach with sparseness constraints, International Computational Engineering 12 (2005) 69.
[28] D.O. Cajueiro, B.M. Tabak, The hurst exponent over time: testing the assertion that emerging markets are becoming more efficient, Physica A 336 (2004) 521–537.
[29] D.O. Cajueiro, B.M. Tabak, Ranking efficiency for emerging markets, Chaos, Solitons and Fractals 22 (2004) 349–352.
[30] K.P. Lim, R. Brooks, The evolution of stock market efficiency over time: a survey of the empirical literature, Journal of Economic Surveys 25 (2011) 69–108.
[31] T. Preis, J.J. Schneider, H.E. Stanley, Switching processes in financial markets, Proceedings of the National Academy of Sciences of USA 108 (2011) 774–7678.